論文 / 著書情報
Article / Book Information

Title	Study of carrier-mobility of organic thin film by dark-injection time-of-flight and electric-field-induced optical second-harmonic generation measurements
Authors	Xin Li, Masashi Sunaga, Dai Taguchi, Takaaki Manaka, Hong Lin, Mitsumasa Iwamoto
Citation	Chemical Physics Letters, 677, 50-54
Pub. date	2017, 3
DOI	http://dx.doi.org/10.1016/j.cplett.2017.03.072
Creative Commons	See next page.
Note	This file is author (final) version.

License

Study of carrier-mobility of organic thin film by dark-injection time-of-flight and electric-field-induced optical second-harmonic generation measurements

Xin Li[1, 2], Masashi Sunaga[1], Dai Taguchi[1], Takaaki Manaka[1], Hong Lin[2] and Mitsumasa Iwamoto[1, *]

1. *Department of Physical Electronics, Tokyo Institute of Technology, 2-12-1 S3-33, O-okayama, Meguro-ku, Tokyo 152-8552, Japan*
2. *State Key Laboratory of New Ceramics & Fine Processing, School of Material Science and Engineering, Tsinghua University, Beijing 100084, China*

*Email iwamoto@pe.titech.ac.jp

Abstract

By using dark-injection time-of-flight (ToF) and time-resolved electric-field-induced optical second-harmonic generation (EFISHG) measurements, we studied carrier mobility μ of pentacene (Pen) thin film of ITO/Pen/Al and Au/Pen/polyimide/ITO diodes where pentacene film is ~ 100 nm in thickness. ToF showed that determination of transit time t_r from trace of transient currents is difficult owing to large capacitive charging current. On the other hand, optical EFISHG is free from this charging current, and allows us to calculate hole and electron mobility as μ_h=1.8×10^{-4} cm^2/Vs and μ_e=7.6×10^{-7} cm^2/Vs, respectively, by using the relation $t_r = d/\mu \int_{t_c}^{t_r} E(0)dt$ (d: Pen thickness, $E(0)$: electric field across Pen), instead of the conventional relationship $t_r = d^2/\mu V$ (V: voltage across Pen). Time-resolved EFISHG measurement is useful for the determination of carrier mobility of organic thin film in

organic devices.

Keywords: electric-field-induced optical second-harmonic generation, carrier transport, carrier mobility, thin film, time-of-flight

1. INTRODUCTION

Organic semiconductor materials have gained extensive attention in electronics over past decades. Considerable interests are attracted not only among scientific community but also in industry, as they possess good processability, mechanical flexibility, and so forth [1]. Using organic semiconductor materials, a variety of organic devices have been designed. Among them are organic light-emitting diodes (OLEDs) [2-4], organic field-effect transistors (OFETs) [5-7], organic solar cells (OSCs) [8-10], and so on. For improving the performance of organic electronic devices, we need to study carrier transport process in devices [11]. Therefore, development of characterization methods for studying carrier transport is important.

Many techniques have been developed to determine carrier mobility in organic films by measuring electrical currents flowing across organic films. These are transient current measurement and steady state current measurement [12-15]. Dark-injection time-of-flight (ToF) and laser-ToF are typical transient measurements, and space charge limited current measurement is a typical steady state current measurement. Using these techniques, the carrier mobility of organic thin film sandwiched between parallel two electrodes has been successfully investigated. As a result, it has been found that the determination of carrier mobility of organic films with a thickness more than 1 μm is well conducted. On the other hand, recent progress in organic electronics motivated us to study carrier mobility of thin active organic layer in organic devices, because carrier behaviors in organic devices differ from those in organic thick films sandwiched between a set of two parallel electrodes.

This motivated us to study the actual carrier mobility of organic semiconductor in organic devices, where the thickness of active organic layer is less than micrometers, e. g., on the order of several hundred nanometers.

In this study, we present time-resolved electric-field-induced optical second-harmonic generation (EFISHG) measurement as an efficient technique of directly visualizing carrier motion in thin films from the electric field point of view [16-19], for the determination of carrier mobility μ of pentacene layer with a thickness of 100 nm and 200 nm in organic diodes. We also use dark-injection ToF measurement for the determination of carrier mobility μ, on the basis of the conventional relationship $t_r = d^2/\mu V$. Here, t_r is carrier transit time, d is the pentacene layer thickness, and V is voltage across the pentacene layer [12, 13]. Noteworthy that ToF is the established electrical measurement used for determining carrier mobility of films [20-24]. In most reported works, the testing film thicknesses is chosen to be over 1 μm, to easily determine the carrier transit time t_r in accordance with the relation $RC \ll t_{tr} \ll \tau_D$. This relation represents the experimental limitations caused by (a) RC response time (RC) and (b) loss of carriers due to deep trapping (τ_D) in transient experiment [25]. On the other hand, in the present study, ToF measurements are tested using diodes with a pentacene layer with a thickness of 100 nm and 200 nm. Results of these ToF and EFISHG measurements are analyzed and the advantage of using EFISHG for determination of carrier mobility of thin organic layer in organic diodes is discussed.

2. EXPERIMENTAL

2.1. Sample preparation

We prepared single-layer diodes with an ITO/pentacene/Al structure and double-layer diodes with an Au/pentacene/polyimide/ITO structure. Figure 1(a) and (b) illustrate these diode structures. For double-layer diodes, a polyimide (PI) layer is used as a carrier blocking layer. This polyimide layer prohibits carriers from crossing the layer, and also blocks carrier injection from the ITO electrode attached.

Samples are prepared as follows; firstly, ITO substrate was pre-cleaned by ultra-sonification (10 min in acetone; 10 min in ethanol; 10 min in deionized water) followed by UV/Ozone dry cleaning. For the deposition of PI layer, 40 wt% CBDA-BAPP (Nissan Chemical Industry) solution was spin-coated (500 rpm for 5 s then 2500 rpm for 25 s) onto the ITO surface, followed by thermal imidization at 260°C for 120 min. The thickness of PI layer was determined using a contact profilometer. Then, pentacene (Tokyo Chemical Industry) was thermally evaporated onto ITO surface (single-layer diode) or on PI surface (double-layer diode) in vacuum (pressure less than 10^{-5} Torr) with a depositing rate of 1 Å/s. Finally, metal electrodes (Au or Al) were deposited by thermal evaporation with a depositing rate of 2 Å/s. The designed electrode area was approximately 3 mm^2. For the vacuum deposition, depositing rate and thickness were controlled by using a quartz crystal microbalance (QCM).

2.2 Time-of-flight measurement

Figure 1(c) shows the setup of ToF measurement. A square-wave voltage with variable amplitude and a settled frequency of 10 Hz was applied to the ITO electrode of diodes in reference to the metal electrode grounded. In experiment, transient electrode charging appeared just after the applied voltage value jumped from 0 V to the target value, and it was followed by carrier injection and succeeding carrier transport. This charging effect must be removed in the measurement. To eliminate the influence of the transient current peak induced by this electrode charging, an external adjustable capacitance C ($\approx C_s$: capacitance of the diode device) and a differential amplifier were installed. The transient current was measured to trace transit of carriers in diode for determining carrier transit time t_r.

2.3 EFISHG measurement

Figure 1(d) shows the experimental setup for EFISHG measurement, and it was the same as that reported in our previous paper [26]. In the way same as in ToF measurement, a square-wave voltage with a frequency of 10 Hz was applied to ITO electrode, to generate carriers that can inject and transport through the pentacene layer. An external optical system is applied to detect time-resolved EFISHG signal. A Q-switched Nd:YAG pulsed laser equipped with a third-harmonic generator and an optical parametric oscillator (OPO) was used as a light source (repetition rate: 10 Hz, pulse duration: 4 ns, average power: 0.6 mW). The EFISHG is a two-photon process and its intensity is given as:

$$I(2\omega) \propto \left|\vec{P}(2\omega)\right|^2,\ \vec{P}(2\omega) = \overleftrightarrow{\chi}^{(3)}(-2\omega; 0, \omega, \omega) : \vec{E}(0)\vec{E}(\omega)\vec{E}(\omega). \quad (1)$$

$\vec{P}(2\omega)$ is the nonlinear polarization induced in organic layers and $\overleftrightarrow{\chi}^{(3)}$ is the third order nonlinear susceptibility tensor. $\vec{E}(0)$ is the electrostatic local field formed in organic layer, and $\vec{E}(\omega)$ is the electric field of incident laser beam. Eq. (1) indicates that the square-root of SHG intensity should be proportional to the magnitude of electric field $\vec{E}(0)$. A principal reason why we can use EFISHG for probing carrier transits is that carriers are a source of this electric field $\vec{E}(0)$ in Eq. (1). $\overleftrightarrow{\chi}^{(3)}$ is activated resonantly at a material-dependent laser wavelength. The wavelength of the pulsed laser was set at 860 nm for probing carrier motion in pentacene layer, and the second-harmonic light intensity $I(2\omega)$ generated at wavelength of 430 nm was probed [27]. Noteworthy that photocarrier generation in pentacene layer is negligible under laser illumination at 860 nm. That is, photoconductivity effect by laser illumination is negligible.

3. RESULTS AND DISCUSSION

3.1 ToF measurement

Figure 2 shows the transient currents measured by ToF. To inject holes and electrons respectively, positive pulse biases (1 V ~ 4 V) are applied to the ITO electrode in single-layer device of ITO/pentacene/Al, while negative biases (-7 V ~ -20 V) are applied to ITO electrode of Au/pentacene/PI/ITO. For each curve, notable current peaks are observed though they appear as a result of overlapping electrode charging with carrier transit. Figure 4(a) plots the time constant τ extracted from the ToF transients by applying the exponential function: $I(t) = I_0 \exp(-(t -$

$t_0)/\tau)$ to fit the decreasing tail (t_0: current peak time for electrode charging). The time constant is plotted as a function of equivalent voltage V_{eq} across the pentacene layer. That is, $V_{eq} = V$ for single-layer diode and $V_{eq} = C_2/(C_1 + C_2) \cdot V$ for double-layer diode (C_1, C_2: capacitance of pentacene and polyimide layer, respectively). In ToF measurements, carrier transport time is voltage-dependent in a manner as $t_r = d^2/\mu V$ and $t_r = 0.786 \times d^2/\mu V$ for space charge free and space charge limited condition, respectively [12]. That is, transport time is inversely proportion to voltage as $t_r \propto 1/V$. By contrast to the $1/V$ dependence, experimentally determined time constant is nearly voltage-independent and governed by the measurement circuit time-constant $RC \sim 10^{-7}$ s. Though we used a differential amplifier to remove the electrode charging current, notable electrode charging dominates the transient currents as electric noise, leading us to a difficult situation in mobility calculation. Further instrumental modification is needed to remove capacitive current in ToF measurement, but it is hard task.

3.2 EFISHG measurement

Figure 3(a) and (b) show time-resolved EFISHG transients of single-layer diode for negative and positive bias, respectively. When the external voltage switched from 0 to V, the detected SHG intensity, proportional to the electric field intensity, increases rapidly with circuit time constant RC, due to electrode charging effect. That is, electrode charges $+Q_m$ and $-Q_m$ are induced on ITO and metal (Au or Al) electrode, respectively, by the external voltage, and change as $\pm Q_m = \pm CV(1 -$

$\exp(-t/RC)$) as expected from electrical circuit analysis [28]. Meanwhile, electric field $E(0)$ is formed in the pentacene layer as $E_m\big(=E(0)\big)=Q_m/\varepsilon$ (ε: dielectric constant of pentacene layer). For negative biases, as shown in Figure 3(a), SHG intensity increases during the electrode charging process and saturates. No obvious SHG intensity decay is observed after the electrode charging, suggesting that the internal electric field intensity remains constant after electrode charging process without further carrier injection. On the other hand, for positive bias, the SHG signal initially increased due to electrode charging, followed by a clear attenuation (for 6 V and 8 V). This is due to hole injection from ITO electrode to pentacene layer, followed by hole transport in the layer. The electric field increases during electrode charging process in the way same as that for negative bias application case. This process is observed as the increase of SHG intensity in Fig. 3(d) at around circuit time constant RC=10^{-7} s. After the electrode charging, electric field E_m is formed in the layer. When carriers inject into the pentacene layer and then transit, these injected carriers form space charge electric field E_s in addition to electrostatic field E_m. In more detail, holes injected from ITO electrode produce space charge field pointing from holes to ITO electrode ($E_s<0$). Accordingly, electric field at the ITO electrode, $E(0)=E_m+E_s$, is decreased. This process resulted in the decrease of SHG intensity by the time hole transport completes at around 10^{-6} s. Figure 4(a) plots the hole transit time t_r determined as the finishing time point of the decay of SHG intensity as a function of the applied voltage V. The transit time is inversely proportion to voltage V, $t_r \propto 1/V$, in a manner as expected from drift carrier motion along electrostatic field

in the film.

Figure 3(c) and (d) illustrate EFISHG results of double-layer diodes for negative and positive bias, respectively. Results showed that, for both positive and negative biases, carrier injection and carrier transit were observed. The SHG intensity increases at RC=10^{-7} s due to electrode charging. Afterwards, SHG signal decays due to carrier injection and transit for both positive and negative biases. This result is different from single-layer diode where the SHG decay related to carrier transport is only observed for hole injection. Taking into account the carrier blocking property of PI layer, we argue that for negative bias the decrease of SHG signal is due to holes injected from Au electrode to pentacene and the decrease in positive bias is due to injected electrons. From the finishing point of SHG signal decay, we extracted hole and electron transit time, and plotted in Fig. 4(a) and (b), respectively, as a function of equivalent voltage $V_{eq} = C_2/(C_1 + C_2) \cdot V$. The result clearly shows that transit time of both holes and electrons are in proportion to reciprocal of voltage $t_r \propto 1/V$ as expected from carrier drift process.

Finally, the time-resolved EFISHG indicated that the local electric field $E(0)$ changed in the pentacene layer with time, due to carrier injection and their transport. The quantitative relation between SHG intensity and electric field intensity $E(0)$ can be determined by measuring the SH-V curves [26, 28, 29]. As the result, for single-layer diode, $E(0) = 6.17 \times \sqrt{SH_t - SH_{base}}/d$ where SH_t is the SHG intensity at the time t, SH_{base} is the signal intensity without external voltage application, and d is the pentacene thickness. Similarly, for double-layer diode,

$E(0) = 32.3 \times \sqrt{SH_t - SH_{base}}/d$. Consequently, by quantitatively fitting the SHG intensity to electric field intensity change, we can calculate carrier mobility μ by using the following relation:

$$\mu = \frac{d}{t_r \int_{t_c}^{t_r} E(0)dt} \quad . \tag{2}$$

t_r is the transit time and t_c(=10^{-7} s) is the starting time point of electrode charging. By using electric field $E(0)$ and Eq. (2), we obtained hole mobility $\mu_h = 1.76 \times 10^{-4}$ cm^2/Vs and electron mobility $\mu_e = 7.59 \times 10^{-7}$ cm^2/Vs from the time-resolved EFISHG measurement for +20 V and -20 V, respectively. It is instructive to point out that the ratio of hole mobility and electron mobility μ_e/μ_h~ 10^{-3} was observed similarly in our previous TRM-SHG experiment of pentacene field-effect transistors [30, 31]. This also supports that the observed carrier mobility is well reflecting carrier transport property of pentacene thin film. The possible origin of low electron mobility is the presence of trapping states in the film due to oxygen and other sources. It is also noteworthy that laser-ToF is another established technique for carrier mobility determination, but it is hard to use this technique for thin film where optical penetration depth exceeds film thickness [12]. Actually, we also carried out the laser ToF for thin film diodes, but it was impossible to determine carrier mobility using the relationship $t_r = d^2/\mu V$. CELIV is another way to extract carrier mobility in thin organic films. This method is useful to eliminate large capacitive current in dark-injection TOF [32-35]. However, injected carriers form electrostatic field and complicates carrier drift motion in transport process, as evidenced by the EFISHG measurement result. Direct probing of electric field in transport process during

transient current measurement is useful to extract carrier mobility with correctly taking account of space charge electric field from injected carriers.

4. Conclusions

EFISHG measurement is employed to analyze carrier transport process in organic thin film (thickness less than 1 μm) and to calculate carrier mobility. The experiment and analysis were compared with conventional ToF measurement. In ToF measurement, carrier transit process and electrode charging process are not quite distinguishable from each other, owing that thin film device allows rather large electrode charging current to be flowed. EFISHG measurement provides clearly distinguished images of electrode charging and carrier transport processes, and allows us to extract carrier mobility. Furthermore, EFISHG measurement demonstrated that injected carriers significantly deform electric field in device, and complicates carrier drift motion. Direct probing of electric field during carrier transport process is useful for extraction of carrier mobility from transient current measurements such as TOF and CELIV where motion of injected carriers are the key to observe transport process.

Acknowledgements

This work was financially supported by a Grant-in-Aid for Scientific Research (S) (Grant No. 22226007) from the Japan Society for the Promotion of Science (JSPS), Japan. L. X. thanks to the Tokyo Tech-Tsinghua University Joint Program.

References

[1] J. M. Shaw and P. F. Seidler, IBM J. Res. Dev. **45**, 3-9 (2001).

[2] J. H. Burroughes, D. D. C. Bradley, A. R. Brown, R. N. Marks, K. Mackay, R. H. Friend, P. L. Burns, and A. B. Holmes, Nature, **347**, 539-541 (1990).

[3] A. Dodabalapur, Solid State Commun. **102**, 259-267 (1997).

[4] B. Geffroy, P. le Roy, and C. Prat, Polymer International **55**, 572- 582 (2006).

[5] G. Horowitz, Adv. Mater.**10**, 365-377 (1998).

[6] M. J. Małachowski, J. Żmija, Opto-Electronics Review **18**, 121-136 (2010).

[7] M. Muccini, Nature Mat. **5**, 605-613 (2006).

[8] Y. J. Cheng, S. H. Yang, C. S. Hsu, Chem. Rev. **109**, 5868–5923 (2009).

[9] S. Günes, H. Neugebauer, N. S. Sariciftci, Chem. Rev. **107**, 1324−1338 (2007).

[10] D. Wöhrle, D. Meissner, Adv. Mater. **3**, 129–138 (1991).

[11] J. L. Brédas, J. P. Calbert, D. A. da Silva Filho, and J. Cornil, Proc. Nat. Acad. Sci. **99**, 5804-5809 (2002).

[12] M. A. Lampert and P. Mark, *Current Injection in Solids* (Academic, New York, 1970).

[13] H. Meier, *Organic Semiconductors -Dark and Photoconductivity of Organic Solids* (Verlag Chemie, Weinheim, 1974).

[14] D. Basu and A. Dodabalapur, Drift velocity and drift mobility measurement in organic semiconductors using pulse voltage, in *Organic Electronics*, Advances in Polymer Science vol 223, edited by G. Meller and T. Grasser (Springer, Heidelberg, 2010).

[15] P. M. Borsenberger and D. S. Weiss, *Organic Photoreceptors for Xerography* (Marcel Dekker, New York, 1998).

[16] T. Manaka, E. Lim, R. Tamura, and M. Iwamoto, Nature Photon. **1**, 581-584 (2007).

[17] M. Iwamoto, T. Manaka, and D. Taguchi, Jpn. J. Appl. Phys. **53**, 100101 (2014).

[18] L. Zhang, D. Taguchi, J. Li, T. Manaka, and M. Iwamoto, Appl. Phys. Lett. **98**, 092109 (2011).

[19] A. Devižis, A. Serbena, K. Meerholz, D. Hertel, and V. Gulbinas, Phys. Rev. Lett. **103**, 027404 (2009).

[20] R. G. Kepler, Phys. Rev. **119**, 1226-1229 (1960).

[21] E. Lebedev, Th. Dittrich, V. Petrova-Koch, S. Karg, W. Brütting, Appl. Phys. Lett. **71**, 2686-2688 (1997).

[22] I. H. Campbell, D. L. Smith, C. J. Neef, and J. P. Ferraris, Appl. Phys. Lett. **74**, 2809-2811 (1999).

[23] P. Cusumano and S. Gambino, J. Electron. Mater. **37**, 231-239 (2008).

[24] M. Funahashi and J. Hanna, Phys. Rev. Lett. **78**, 2184-2187 (1997).

[25] H. Scher, Phys. Rev. B **12**, 2455-2477 (1975).

[26] D. Taguchi, M. Weis, T. Manaka, and M. Iwamoto, Appl. Phys. Lett. **95**, 263310 (2009).

[27] J. Li, L. Zhang, W. Ou-Yang, D. Taguchi, T. Manaka, and M. Iwamoto, Jpn. J. Appl. Phys. **49**, 121601 (2010).

[28] D. Taguchi, L. Zhang, J. Li, M. Weis, T. Manaka, and M. Iwamoto, J. Phys. Chem. C, **114**, 151136-15140 (2010).

[29] D. Taguchi, T. Manaka, and M. Iwamoto, Jpn. J. Appl. Phys. **55**, 03DC04 (2016).

[30] T. Manaka, M. Nakao, E. Lim, and M. Iwamoto, Material Science-Poland **27**, 709-717 (2009).

[31] M. Iwamoto, T. Manaka, and D. Taguchi, J. Phys. D: Appl. Phys. **48**, 373001/1-20 (2015).

[32] G. Juška, K. Arlauskas, and M. Viliūnas, Phys. Rev. Lett. **84**, 4946-4949 (2000).

[33] A. Pivrikas, N. S. Sariciftci, G. Juška and R. Österbacka, Prog. Photovolt: Res. Appl. **15**, 677–696 (2007).

[34] J. Schafferhans, A. Baumann, A. Wagenpfahl, C. Deibel and V. Dyakonov, Org. Electron. **11**, 1693–1700 (2010).

[35] G. Juška, K. Genevičius, M. Viliunas, K. Arlauskas, H. Stuchlíková, A. Fejfar and J. Kočka, J. Non-Cryst. Solids, **266-269**, 331-335 (2000).

Figure captions

Figure 1: Sample structure of (a) single-layer ITO/pentacene (Pen)/Al, (b) double-layer Au/Pen/polyimide (PI)/ITO diodes. Experimental setup for (c) ToF and (d) EFISHG measurements.

Figure 2: ToF results of (a) ITO/Pen/Al diode, (b) Au/Pen/PI/ITO diode.

Figure 3: EFISHG results for ITO/Pen/Al diode by applying (a) negative voltage, (b) positive voltage. The results for Au/Pen/PI/ITO diode under (c) positive voltage, (d) negative voltage application.

Figure 4: Transit time extracted from ToF (filled symbols) and EFISHG (open symbols) measurements for single-layer (square symbol) and double-layer (circular symbol) diodes. (a) Hole transit. (b) Electron transit.

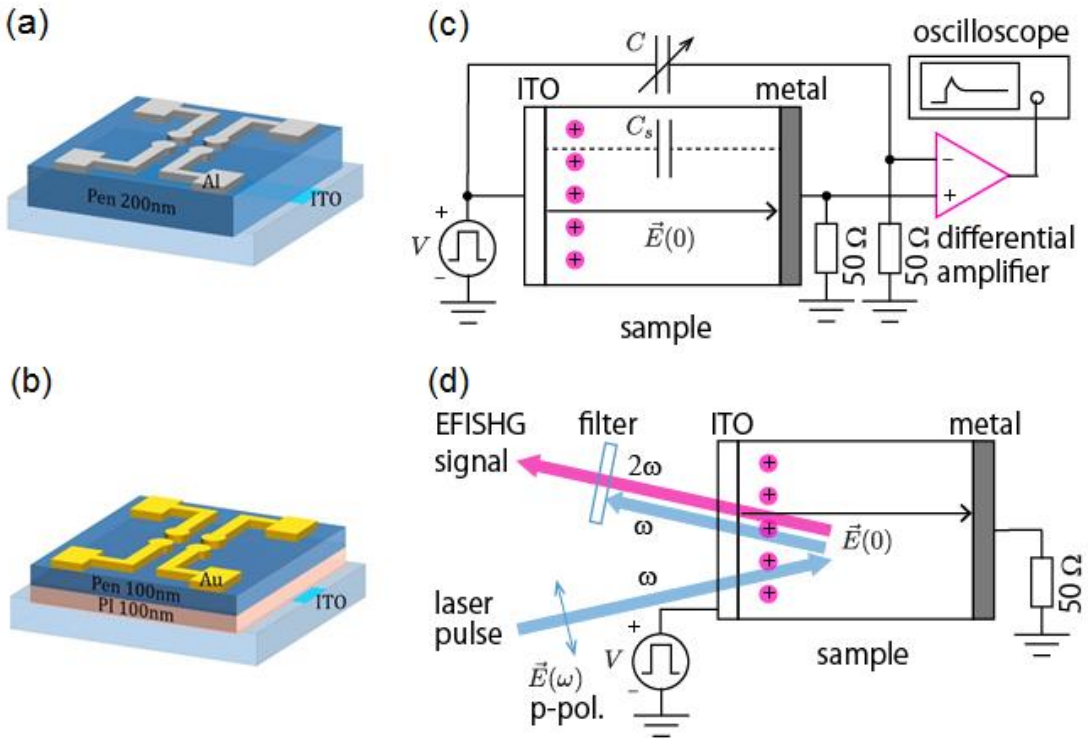

Figure 1: Xin Li et al.

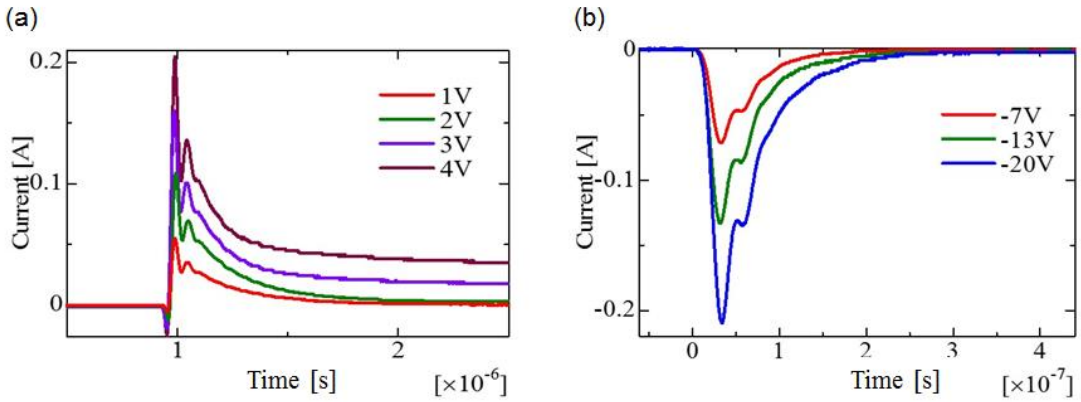

Figure 2: Xin Li et al.

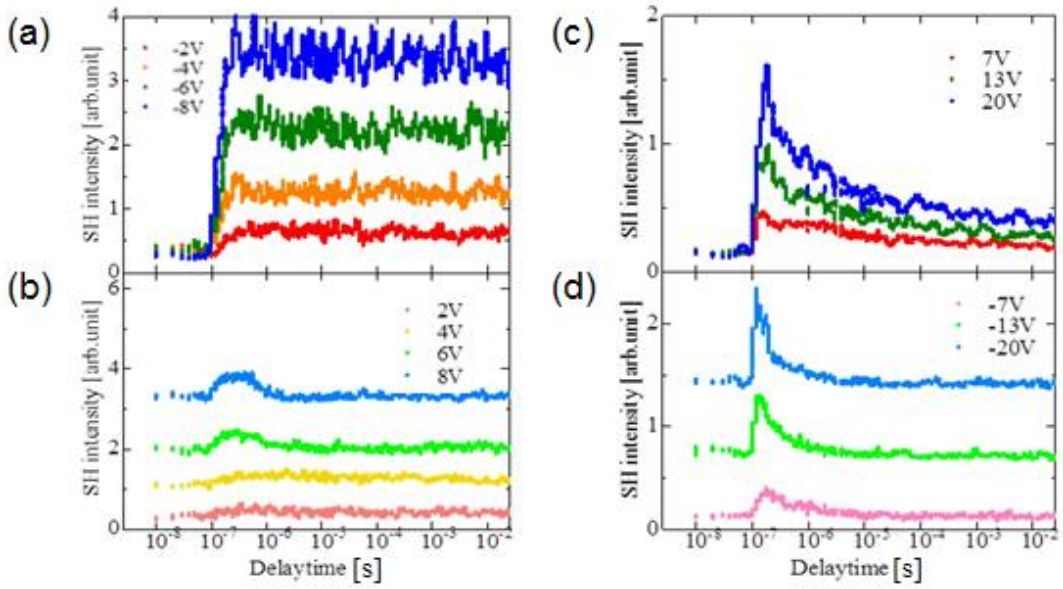

Figure 3: Xin Li et al.

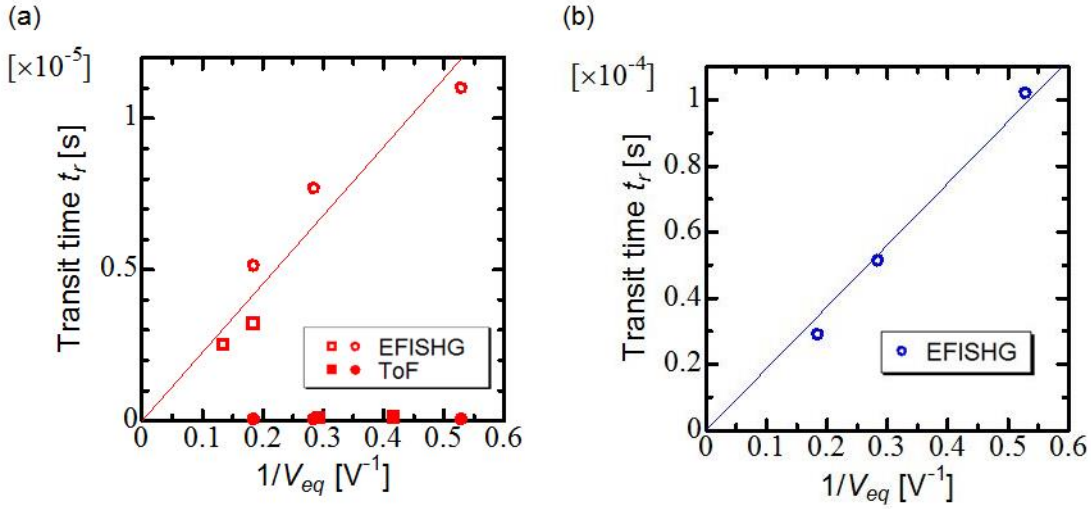

Figure 4: Xin Li et al.